Proton Transfers in the β-Reaction Catalyzed by Tryptophan Synthase[†]

Oscar Hur, Dimitri Niks, Patricia Casino, and Michael F. Dunn*

Department of Biochemistry, University of California, Riverside, California 92521

Received January 22, 2002; Revised Manuscript Received May 29, 2002

ABSTRACT: Reactions catalyzed by the β-subunits of the tryptophan synthase $\alpha_2\beta_2$ complex involve multiple covalent transformations facilitated by proton transfers between the coenzyme, the reacting substrates, and acid−base catalytic groups of the enzyme. However, the UV/Vis absorbance spectra of covalent intermediates formed between the pyridoxal 5′-phosphate coenzyme (PLP) and the reacting substrate are remarkably pH-independent. Furthermore, the α-aminoacrylate Schiff base intermediate, E(A−A), formed between L-Ser and enzyme-bound PLP has an unusual spectrum with $\lambda_{max} = 350$ nm and a shoulder extending to greater than 500 nm. Other PLP enzymes that form E(A−A) species exhibit intense bands with $\lambda_{max} \sim 460-470$ nm. To further investigate this unusual tryptophan synthase E(A−A) species, these studies examine the kinetics of H^+ release in the reaction of L-Ser with the enzyme using rapid kinetics and the H^+ indicator phenol red in solutions weakly buffered by substrate L-serine. This work establishes that the reaction of L-Ser with tryptophan synthase gives an H^+ release when the external aldimine of L-Ser, $E(Aex_1)$, is converted to E(A−A). This same H^+ release occurs in the reaction of L-Ser plus the indole analogue, aniline, in a step that is rate-determining for the appearance of $E(Q)_{Aniline}$. We propose that the kinetic and spectroscopic properties of the L-Ser reaction with tryptophan synthase reflect a mechanism wherein the kinetically detected proton release arises from conversion of an $E(Aex_1)$ species protonated at the Schiff base nitrogen to an E(A−A) species with a neutral Schiff base nitrogen. The mechanistic and conformational implications of this transformation are discussed.

The families of enzymes that utilize pyridoxal 5′-phosphate (PLP)[1] as coenzyme catalyze a diversity of chemical reactions unmatched by any other coenzyme (*1*−*8*). These reactions typically involve several covalent intermediates formed between PLP and the reacting substrate(s), including tetrahedral adducts (gem diamines), Schiff base intermediates (aldimines and ketamines), α-aminoacrylyl Schiff base intermediates, and quinonoid intermediates. These intermediates participate in a wide variety of bond scission/bond formation processes, including C−H, N−H, O−H, C−C, C−O, C−N, C−S, and C−Se bonds. Scheme 1A shows the covalent intermediates in the tryptophan synthase catalytic mechanism. The processes shown in Scheme 1A require acid−base catalysis involving proton transfers between the reacting substrate and/or the coenzyme that are mediated by catalytic residues at the active site.

The enzyme-bound PLP moiety (Scheme 1B) is comprised of four groups capable of ionization in the physiological pH range: the pyridine ring N-1, the ring hydroxyl at C-3, the ubiquitous Schiff bases at C-4′, and the phosphoryl group at C-5′. The chemical properties of the PLP moiety are critically dependent on the ionization states of these groups. For example, the protonation state of the Schiff base linkage at C-4′ modulates the reactivity of the C-4′ carbon toward nucleophilic attack (*8*). The conversion of Schiff base species to quinonoid species is dependent on protonation at N-1, and the state of protonation of N-1 modulates the pK_a of the Schiff base nitrogen. The state of protonation of the C-3 hydroxyl modulates the reactivity and protonation state of the Schiff base nitrogen (*9*−*11*). The state of protonation of the 5′-phosphoryl group is important for binding (*12*).

In most PLP enzymes, the ionizable groups of the coenzyme are buried within the protein (*13*−*19*). The pK_as of these groups are strongly influenced by the microenvironment provided by the protein, and in some instances the microenvironment locks the group into a single ionization state that persists over the physiological pH range (pH 6−10). In other instances, the microenvironment at the site makes possible a switching between ionization states during the catalytic cycle.

[†] Supported by NIH Grant GM55749.

* Correspondence should be addressed to this author. Phone: 909-787-4235, Fax: 909-787-4434, E-mail: michael.dunn@ucr.edu.

[1] Abbreviations: $\alpha_2\beta_2$, native form of tryptophan synthase from *S. typhimurium*; α, alpha subunit; β, beta subunit; E(Ain), internal aldimine (Schiff base); $E(Aex_1)$, external aldimine intermediate formed between the PLP cofactor and L-Ser; $E(Aex_1)H^+$, external aldimine protonated at the Schiff base nitrogen; E(GD), gem diamine species; E(A−A), α-aminoacrylate Schiff base; $E(A-A)H^+$, α-aminoacrylate protonated at the Schiff base nitrogen; $E(Q_3)$, quinonoid intermediate that accumulates during the reaction between E(A−A) and indole; $E(Q)_{Aniline}$, quinonoid species derived from the reaction of aniline with E(A−A); $E(Aex_2)$, L-Trp external aldimine; PLP, pyridoxal phosphate; L-Ser, L-serine; L-Trp, L-tryptophan; IGP, 3-indole-D-glycerol 3′-phosphate; GP, α-glycerol phosphate; G3P, glyceraldehyde 3-phosphate; TEA, triethanolamine; $1/\tau_n$, apparent first-order rate constant of the *n*th relaxation; A_n, amplitude of the *n*th relaxation; MVC, monovalent cation.

10.1021/bi025568u CCC: $22.00
Published on Web 07/13/2002

Scheme 1[a]

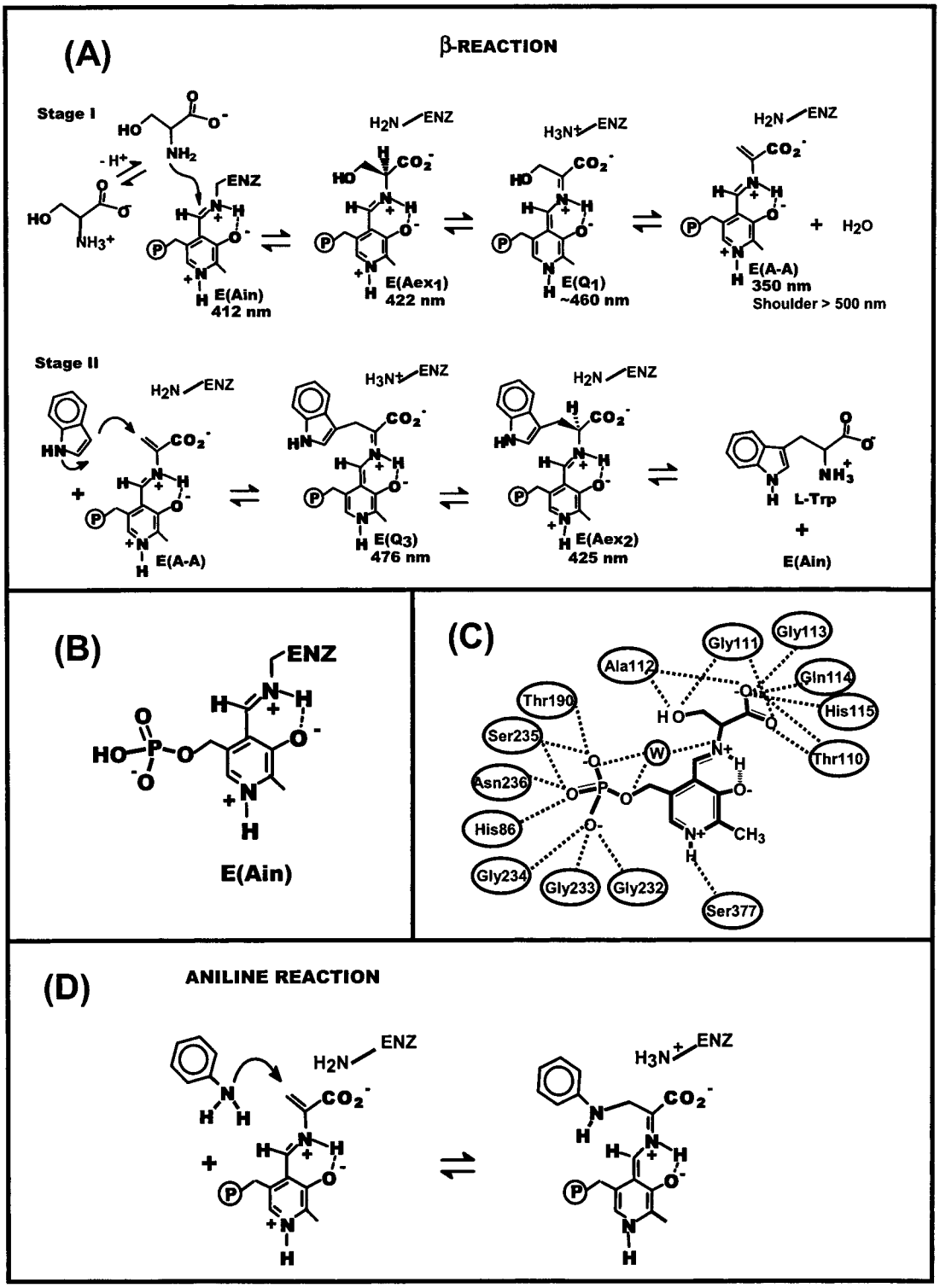

[a] (A) Organic structures of reactants, products, and intermediates identified in the tryptophan synthase β-reaction. (B) Structure of an internal aldimine with the Schiff base and pyridine ring nitrogens protonated. (C) Hydrogen bonding scheme for the tryptophan synthase L-Ser external aldimine, E(Aex_1), formed with the K87T mutant from the X-ray structure (*15*). Redrawn from Rhee et al. (*15*). (D) Reaction of the indole analogue aniline with the α-aminoacrylate Schiff base intermediate to form $E(Q)_{Aniline}$.

Owing to the chromophoric properties of the PLP moiety, the switching among covalent states and ionization states is accompanied by distinctive changes in the UV/Vis absorption spectrum. However, due to the potential complexity of the spectrum arising from the microenvironment and the potential for multiple ionization states, it has not been easy to assign ionization states from examination of the electronic absorption spectrum (*8*, *20*−*25*).

It is now well established that the pH dependencies of the spectra of the E(Ain) and E(Aex) species of the transaminases

and tryptophanase arise from the ionization of the protonated Schiff base linkages of these species (eq 1).

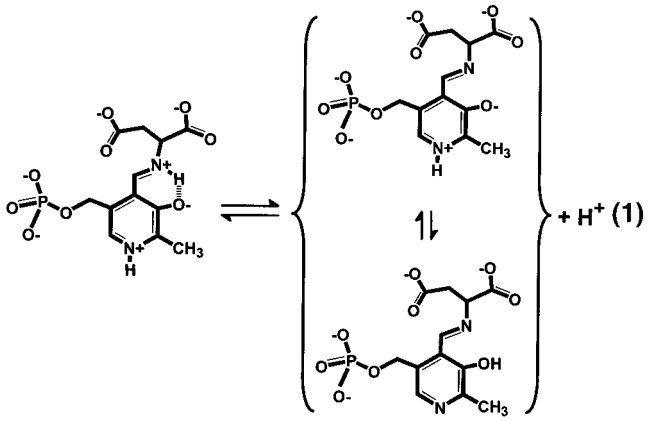

In the E(Ain) species of aspartate aminotransaminase, AAT, this ionization shifts the absorption spectrum from 415 to 360 nm, while in the E(Aex) species, the shift is from 420 to 380 nm (*26*−*29*). Yano et al. (*9*) and Onuffer and Kirsch (*10*) have shown that in AAT the pK_a of the Schiff base nitrogen is modulated by the protonation state of the PLP pyridine ring N-1. In native AAT, the residue that interacts with the pyridine ring N-1 is Asp 222. Mutation of this residue to Ala or Asn renders the spectrum of the internal aldimine (λ_{max} 430 nm) pH-independent, presumably as a consequence of perturbation of the Schiff base nitrogen to a pK_a value outside the physiological range.

In contrast to this behavior, the tryptophan synthase E(Ain), with λ_{max} 412 nm, and the E(Aex$_1$) species, with λ_{max} 424 nm, are essentially pH-independent in the pH range 6−10.4 (*30*−*32*), indicating that the microenvironment of the β-site locks each of these species into a single ionization state where the Schiff base nitrogen is protonated (Scheme 1C).[2] This pH independence is abolished when Ser 377, the residue that interacts with the PLP pyridine ring nitrogen, is replaced by Asp or Glu (*33*). In the Asp mutant, the absorption spectrum of the internal aldimine becomes pH-dependent, shifting from 416 to 336 nm, reflecting protonation/deprotonation of the Schiff base nitrogen. Jhee et al. (*33*) propose that the substitution of Ser 377 by Asp raises the pK_a of the PLP N-1 by 2−5 pK_a units, and reduces the pK_a of the Schiff base nitrogen ∼2.5 units, thereby bringing the pK_as of these nitrogen atoms into the physiological range.

The PLP enzymes cystathionine β-synthase (*34*) and *O*-acetyl-L-serine sulfhydrylase (*35*−*38*) are both involved in β-replacement reactions. These enzymes form α-aminoacrylate Schiff base intermediates, E(A−A), which give UV/Vis absorption spectra with a coenzyme λ_{max} ∼ 460−470 nm. The spectrum of the *O*-acetyl-L-serine sulfhydrylase α-aminoacrylate intermediate is reported to be pH-independent over the range 5.5−9.0 (*39*). The tryptophan synthase α-aminoacrylate has been assigned a UV/Vis spectrum consisting of a coenzyme λ_{max} = 350 nm with a shoulder extending to >500 nm (*23*, *24*, *40*−*42*) that is essentially pH-independent over the pH region 6.5−9.5 (*32*). The binding of Cs^+ to the monovalent cation sites on the β-subunit perturbs this spectrum, forming a long-wavelength maximum at ∼460 nm of apparent low intensity (*43*). While the spectra of the tryptophan synthase internal aldimine, external aldimine, and α-aminoacrylate Schiff base species are not influenced by pH changes in the neutral to basic range, the distribution of these species (formed in Stage I of the β-reaction, Scheme 1A), especially the external aldimine and α-aminoacrylate species, show a marked dependence on pH, with acidic pH favoring the α-aminoacrylate and basic pH favoring the external aldimine (*31*, *32*). This pH-dependent redistribution of chemical intermediates reflects a pH-dependent modulation of the conformation states of the β-subunit (*31*, *32*).

While the spectra of key intermediates in the β-reaction of tryptophan synthase are insensitive to pH in the range 6−10, the chemical steps depicted in the catalytic cycle (Scheme 1A) require several proton transfers. To further investigate the relationship between the spectral changes that occur during the β-reaction, the chemical mechanism of catalysis, and the allosteric transformations that regulate channeling, we have undertaken rapid kinetic investigations of H^+ uptake and/or release both during the reaction of L-Ser (Stage I of the β-reaction, Scheme 1A) and during the reaction of L-Ser and an indole analogue, aniline (Scheme 1D), at the β-site (*44*−*46*). These studies show that the interconversion of the tryptophan synthase external aldimine and α-aminoacrylate species is accompanied by release of a proton, and that the α-aminoacrylate species with λ_{max} = 350 nm is the neutral form of the Schiff base linkage.

MATERIALS AND METHODS

Materials. Aniline hydrochloride (Mallinckrodt), triethanolamine (Aldrich), [α-^{2}H]-L-Ser (Cambridge Isotope Laboratories), phenol red (Aldrich), liver alcohol dehydrogenase (Boehringer Mannheim), bovine carbonic anhydrase (Worthington), and L-Ser were purchased as the highest purity materials available and used without further purification.

Purification of wild-type tryptophan synthase from *Salmonella typhimurium* was performed as previously described (*47*−*51*). Except where noted, all experiments were carried out in solutions containing 100 mM NaCl to ensure that the enzyme was maintained in the Na^+ form (*52*).

UV−*Vis Absorbance Measurements.* Absorbance spectra and activity measurements were performed on a Hewlett-Packard 8452 diode array spectrophotometer at 25 ± 2 °C. Spectra were fitted to sums of log-normal curves as previously described (*25*, *52*−*55*).

Single-Wavelength Stopped-Flow (SWSF) Kinetic Studies. SWSF measurements were performed as previously described at 25 ± 2 °C (*50*, *51*). Kinetic time courses were fitted by nonlinear least-squares regression analysis using the software Peakfit (version 4, Jandel Scientific) to a sum of exponentials according to eq 2:

$$A = A_\infty \pm \Sigma_i A_i \exp(t/\tau_i) \qquad (2)$$

where A_t is the absorbance at time t, A_∞ is the final absorbance, A_i is the absorbance due to the ith relaxation, and $1/\tau_i$ corresponds to the observed rate for the ith relaxation.

[2] The pH dependencies of the steady-state kinetic parameters have not been published for the *S. typhimurium* tryptophan synthase; hence, very little is known about the dependence of K_m and k_{cat} for the α, β, and αβ reactions.

Kinetics of Proton Release. The solutions used in these studies were weakly buffered with substrate L-Ser as the predominating buffer component (1 mM after mixing in the stopped-flow apparatus). The determination of the SWSF time courses for proton release (*56*, *57*) during the reaction of 1 mM L-Ser (Stage I of the β-reaction) and the reaction of 1 mM L-Ser plus 4 mM aniline with tryptophan synthase was carried out in degassed solutions. The solutions were adjusted to pH 7.8 by the addition of NaOH just prior to introduction into the stopped-flow apparatus. This L-Ser concentration is sufficient to saturate binding and reaction in Stage I at pH 7.8. Typically, one syringe of the stopped-flow apparatus contained 44 μM tryptophan synthase, 25 μM phenol red, 100 mM NaCl, and 0.1 mg/mL carbonic anhydrase. The second syringe contained identical concentrations of phenol red, NaCl, and carbonic anhydrase. The second syringe also contained either 2 mM L-Ser or 2 mM L-Ser and 8 mM aniline, as required by the particular experiment. In the absence of strong catalysts, relaxations due to the hydration of CO_2 as per eq 3:

$$CO_2 + H_2O \rightleftharpoons HCO_3^- + H^+ \qquad (3)$$

can give proton concentration changes on time scales comparable to the tryptophan synthase catalyzed reactions under study in this work. Therefore, carbonic anhydrase was added to both syringes to ensure that the reaction of any dissolved CO_2 with water to give HCO_3^- and H^+ reached equilibrium on time scales that were rapid relative to the tryptophan synthase catalyzed reactions under study (*58*). Consequently, any mismatching of the concentrations of CO_2 and HCO_3^- in the two syringes prior to mixing was brought to equilibrium within the experiment mixing dead-time via carbonic anhydrase catalysis.

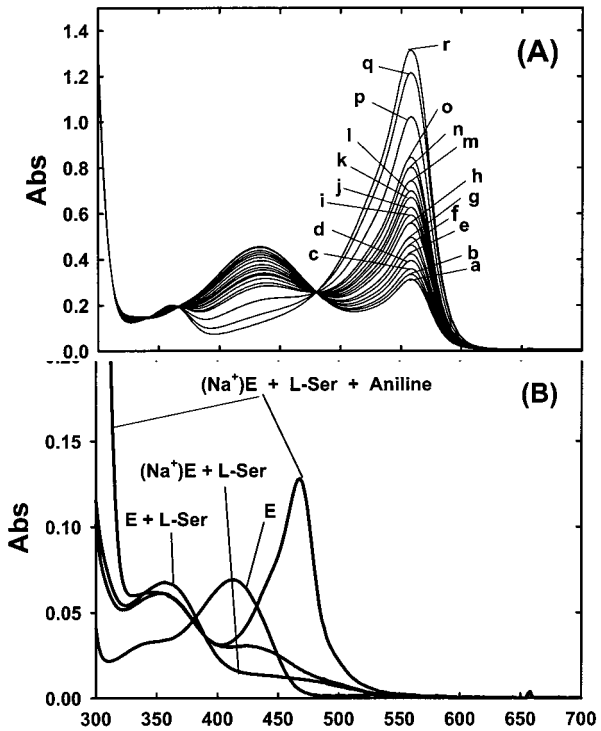

FIGURE 1: Comparison of the pH-dependent changes in the UV/Vis absorption spectrum of phenol red (A) with the spectra of tryptophan synthase intermediates formed in the reaction of the enzyme with L-Ser and with L-Ser and aniline (B). Spectra in (A) were recorded at 25 ± 2 °C for solutions containing 20 μM phenol red at pH values of (a) 7.15, (b) 7.20, (c) 7.25, (d) 7.29, (e) 7.34, (f) 7.39, (g) 7.44, (h) 7.50, (i) 7.55, (j) 7.59, (k) 7.64, (l) 7.68, (m) 7.72, (n) 7.79, (o) 7.83, (p) 8.07, (q) 8.35, and (r) 8.55. Isosbestic points are located at 340, 480, and 560 nm. The spectra in (B) were obtained by reaction of 10 mM tryptophan synthase with 40 mM L-Ser in the presence or absence of 100 mM Na^+, or in the presence of 40 mM L-Ser, 100 mM Na^+, and 4 mM aniline. The spectrum of 10 μM enzyme is also shown.

RESULTS

Comparison of the Phenol Red Spectrum with the Spectra of Tryptophan Synthase Intermediates. In the experiments conducted in this study, a pH indicator dye (phenol red) was used to measure proton release/uptake during reactions at the β-site of the tryptophan synthase bienzyme complex (*56*). The solutions were weakly buffered, with the dominating buffering capacity contributed by the 1 mM L-Ser present as substrate. To maintain ionic strength and to maintain the enzyme in the activated, Na^+ form, reactions were run in the presence of 100 mM NaCl.

Under the experimental conditions used, phenol red has a pK_a value of ~7.8. The acidic (protonated) form of phenol red with λ_{max} at 434 nm exhibits a yellow color, whereas the basic (unprotonated) form with λ_{max} at 560 nm exhibits an intense red color. Figure 1A compares the phenol red spectrum at pH values from 7.15 to 8.55 with the spectra of the tryptophan synthase system (Figure 1B). These spectra consist of the Na^+ form of the internal aldimine Schiff base, the equilibrating mixture of the L-Ser external aldimine, the α-aminoacrylate derived from reaction of the internal aldimine with L-Ser, the α-aminoacrylate formed in the absence of monovalent cations (MVCs), and the aniline quinonoid species generated from reaction of aniline with the α-aminoacrylate (Figure 1B). The phenol red spectra show the presence of isosbestic points located at 340, 370, and 480 nm. The isosbestic points located at 340 and 480 nm are nicely positioned for monitoring the interconversion of the external aldimine and the α-aminoacrylate and also the formation of $E(Q)_{Aniline}$ in the presence of phenol red, without the complication of contributions from the interconversion of the acidic and basic forms of phenol red.

Phenol Red Changes during the Reaction of L-Ser with $\alpha_2\beta_2$ in a Weakly Buffered Solution. When L-Ser reacts with the Na^+ form of tryptophan synthase, the time course of the reaction consists of the appearance and decay of the external aldimine Schiff base species (λ_{max} = 425 nm) and the appearance of the α-aminoacrylate Schiff base species (λ_{max} = 350 nm with a shoulder extending beyond 500 nm, Figure 1B) (*23*). The formation of the external aldimine in the reaction of L-Ser with the internal aldimine form of the enzyme is very fast (>100 s^{-1} under these conditions), while the conversion of the external aldimine to the α-aminoacrylate is slower (~5−7 s^{-1}) (*51*, *59*). Figure 2 compares time courses for the conversion of the extenal aldimine to the α-aminoacrylate measured at 340 nm, with the changes in the phenol red spectrum measured at 560 nm in solutions where substrate L-Ser (1 mM after mixing in the stopped-flow apparatus) also serves as the predominating buffer species. Solutions were adjusted to pH 7.8 with NaOH just prior to introduction into the stopped-flow apparatus. Owing to the rapid rate of formation of the external aldimine and the small change in extinction coefficient at 340 nm, only a

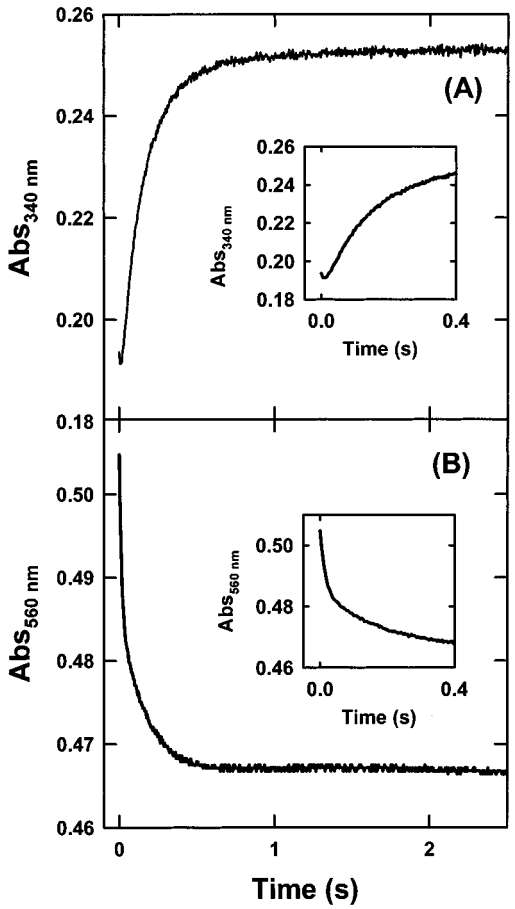

FIGURE 2: Stopped-flow rapid-mixing time courses for the conversion of $E(Aex_1)$ to E(A−A) measured under weakly buffered conditions in 100 mM NaCl at pH 7.80. The traces compare the changes at 340 nm (A) with the changes in the phenol red spectrum measured at 560 nm (B). The insets to each panel show the initial portion of each trace on an expanded time scale. Conditions: one syringe contained 44 μM tryptophan synthase. The second syringe contained 2 mM L-Ser. Both syringes contained 25 μM phenol red, 100 mM NaCl, and 0.1 mg/mL carbonic anhydrase.

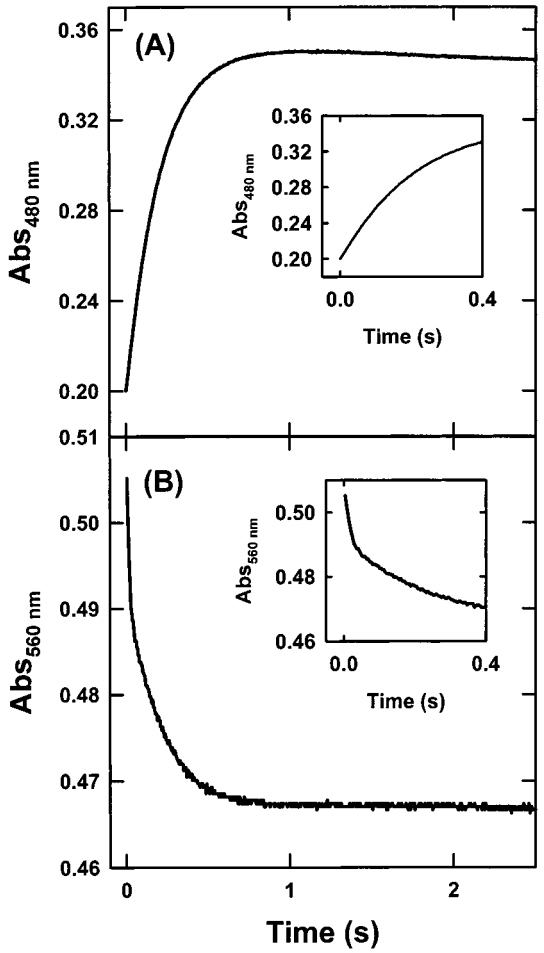

FIGURE 3: Comparison of stopped-flow rapid-mixing time courses for the reaction of 22 μM tryptophan synthase with 1 mM L-Ser and 4 mM aniline under weakly buffered conditions measured at 480 nm (A) and at 560 nm (B) carried out in the presence of 25 mM phenol red and 100 mM NaCl. The insets in each panel show the initial portions of the time courses on expanded time scales. Conditions were the same as those described in Figure 2 except that both 2 mM L-Ser and 8 mM aniline were present in the substrate syringe.

hint of this process is detectable as an initial fast phase in these time courses. The pH-dependent spectrum of phenol red exhibits an isosbestic point at 340 nm (Figure 1); therefore, time courses measured at this wavelength only show contributions from changes in the PLP absorption spectrum. The time courses at 560 and 340 nm show similar kinetic behavior. The 340 nm time course exhibits a rapid phase of decreasing absorbance and a very small apparent amplitude corresponding to the conversion of the internal aldimine to the external aldimine (Figure 2A inset). The small amplitude of this relaxation prevented estimation of its relaxation rate. This phase is followed by a relaxation of increasing absorbance with a much greater amplitude. This slower relaxation could be fitted to the expression for a single exponential (eq 2) with a rate of $5.6 \pm 0.8\ s^{-1}$. The 560 nm time course shows two phases of decreasing absorbance; the faster phase gave a relaxation rate of $\sim 140\ s^{-1}$; the slower phase gave a relaxation rate of $8.0 \pm 0.6\ s^{-1}$.

Phenol Red Changes during the Reaction of L-Ser and Aniline with $\alpha_2\beta_2$ in a Weakly Buffered Solution. The Na^+ form of tryptophan synthase reacts with L-Ser to form a quasi-equilibrium between the L-Ser external aldimine and the α-aminoacrylate species. The α-aminoacrylate species reacts rapidly with indole and indole analogues to form quinonoid species that may be converted to final products (L-Trp or an L-Trp analogue). However, when the nucleophilic analogue aniline is used in place of indole, reaction stops at the aniline quinonoid intermediate, $(Na^+)E(Q)_{Aniline}$, and no detectable new amino acid is formed with the wild-type enzyme (*44*). Consequently, when L-Ser and aniline are rapidly mixed with tryptophan synthase, the time course consists of the formation of the α-aminoacrylate, which then is converted to $(Na^+)E(Q)_{Aniline}$. Because the reaction of aniline with the α-aminoacrylate is considerably faster than the conversion of the external aldimine to the α-aminoacrylate, this latter process is rate-determining for the appearance of $(Na^+)E(Q)_{Aniline}$ (*44*, *60*−*63*). The time courses for this reaction measured at 480 nm and at 560 nm carried out in the presence of phenol red are shown in Figure 3A,B. In agreement with previous observations, the 480 nm time course (Figure 3A) consists of a monophasic increase in absorbance ($1/\tau = 5.5 \pm 0.7\ s^{-1}$), followed by a much slower relaxation of small amplitude. The 560 nm time course (Figure 3B) occurs in two kinetic phases of similar amplitude.

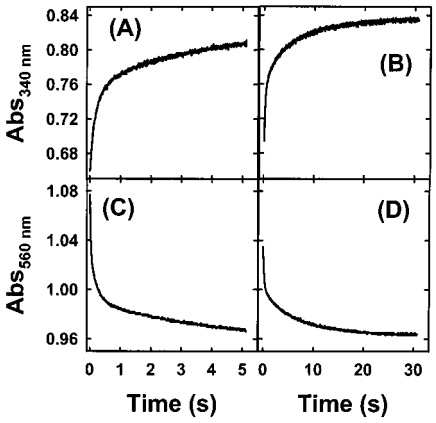

FIGURE 4: Quantification of proton release. Time courses for the reaction of L-Ser with tryptophan synthase in the presence of phenol red were measured under weakly buffered conditions as described in Figure 2, but with the presence of liver alcohol dehydrogenase (LADH) and NAD^+ in one syringe of the stopped-flow apparatus and ethanol in the other. The traces measured in (A) and (B) compare the 340 nm absorbance changes for 5 and 30 s, respectively, with the traces measured at 560 nm (C and D) on the same time scales. While the initial, faster phase observed in each trace at 340 nm is contributed by the reaction of tryptophan synthase with L-Ser, the slower phase arises from the conversion of NAD^+ to NADH resulting from the oxidation of ethanol. The time courses measured at 560 nm show the phenol red changes measured in the same solutions. The final concentrations used were as follows: 22 μM tryptophan synthase; 1 mM L-Ser; 25 μM phenol red; 100 mM NaCl; 0.1 mg/mL carbonic anhydrase; 0.7 mg/mL alcohol dehydrogenase; 30 mM NAD^+; and 120 mM ethanol.

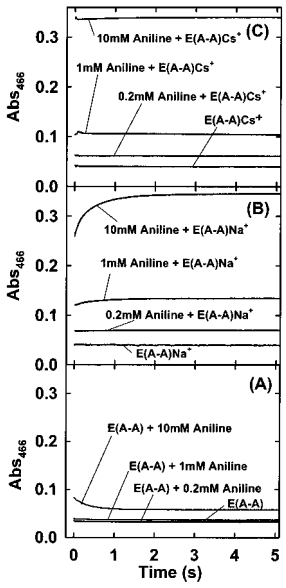

FIGURE 5: Rapid-mixing stopped-flow time courses comparing the reactions of the MVC-free (A), Na^+ (B), and Cs^+ (C) forms of the α-aminoacrylate with the indole analogue, aniline, in 50 mM TEA buffer at pH 7.80 and 25 ± 2.0 °C. In each panel, 40 μM tryptophan synthase was preincubated with 40 mM L-Ser in one syringe and then mixed in the stopped-flow apparatus with 40 mM L-Ser and either 20 (a), 2 (b), or 0.4 mM (c) mM aniline in the other syringe. In (A), both syringes contained 100 mM NaCl, while in (B), both syringes contained 100 mM CsCl. The background absorbance (trace d) was determined in each experiment by mixing the syringe containing enzyme and L-Ser with buffer.

The faster relaxation has a rate of >50 s^{-1}, whereas the slower relaxation has a rate of 4.1 ± 0.5 s^{-1}. The yield of H^+, as measured by the amplitude of the phenol red signal in the slow phase, is essentially the same as that detected in the reaction of L-Ser alone (Figure 2).

The 480 and 560 nm time courses for the reaction of L-Ser and aniline with tryptophan synthase also were measured in the presence of phenol red, but in a strongly buffered solution. The time course at 480 nm for the formation of $(Na^+)E(Q)_{Aniline}$ (data not shown) consisted of a single relaxation with $1/\tau = 5.7 \pm 0.6$ s^{-1}, a value in reasonable agreement with the value of the slow relaxation obtained in Figure 3A. The 560 nm time course (data not shown) exhibited no change in absorbance over the 2 s period of observation. This control experiment establishes that the 560 nm changes observed in (B) have their origins in a proton release reaction.

Quantification of the Amount of Proton Release. To determine the correlation between the absorbance changes at 560 nm with the amount of proton release, the following experiment was conducted. Reaction of 1.0 mM L-Ser with 22 μM tryptophan synthase in the presence of 25 μM phenol red was carried out under the same weakly buffered conditions used in Figures 2 and 3, but containing, in addition, 0.7 mg/mL liver alcohol dehydrogenase (LADH) and 30 μM NAD^+ in one syringe of the stopped flow and 20 mM ethanol in the other (Figure 4). The mixing of LADH and NAD^+ with ethanol under experimental conditions such as those used in Figure 4 gives reaction to form NADH, acetaldehyde, and a proton with a 1:1:1 stoichiometry (*56*, *64*). The time courses at 340 nm and at 560 nm are shown for two different time scales in Figure 4A,B and Figure 4C,D, respectively. The concentration of LADH was selected to give a rate of production of H^+ that was slow relative to the relaxations observed in the reaction of L-Ser with tryptophan synthase. These slow kinetic processes give rise to the slow absorbance increase at 340 due to NADH production in panels A and B and to the slow absorbance decrease at 560 nm due to H^+ production in panels C and D. Comparison of the absorbance changes for the appearance of NADH measured at 340 nm with the slow absorption changes at 560 nm establishes the relationship between the net proton change and the net absorption change measured at 560 nm. Amplitude analysis of the time courses presented in Figure 4 shows that a 0.035 ± 0.005 change in absorbance at 560 nm corresponds to a 9.60 ± 0.8 μM change in the concentration of NADH, and therefore a 9.60 ± 0.8 μM change in H^+. Therefore, a 0.08 ± 0.01 change in absorbance at 560 nm attributed to the tryptophan synthase reaction (the faster phase in Figure 4C) corresponds to the release of ~22 μM H^+. This yield gives a stoichiometry ratio of ~(22 μM H^+)/(44 μM β-sites) = ~0.5 mol of H^+/mol of β-site.

Comparison of the Monovalent-Cation-Free, Na^+ and Cs^+ Forms of Tryptophan Synthase in the Reaction with L-Ser and Aniline. Figure 5 compares the time courses for the reactions of the monovalent-cation-free (MVC-free), Na^+ and Cs^+ forms of tryptophan synthase with L-Ser and aniline. In these experiments, tryptophan synthase was preincubated with 40 mM L-Ser prior to mixing with either 10, 1, or 0.2 mM aniline so that the reactions of the corresponding MVC-free (Figure 5A), Na^+ (Figure 5B) and Cs^+ forms (Figure 5C) of the α-aminoacrylate species could be directly compared. With 10 mM aniline, both the Na^+ and Cs^+ forms give high yields of $E(Q)_{Aniline}$, whereas the MVC-free

α-aminoacrylate gives a much smaller yield of $E(Q)_{Aniline}$ (~16.5% of the total yield obtained with the Na^+ or Cs^+ forms; compare Figure 5A, 5B, and 5C). This low yield reflects the deactivated state of the MVC-free enzyme (*50*−*52*, *59*). The MVC-free system gives a burst reaction that is complete in the mixing dead time, followed by a decay phase that reduces the amount of $E(Q)_{Aniline}$ formed by about 50%. As is evident in Figure 5B,C, the Na^+ and Cs^+ forms of the α-aminoacrylate give similarly high yields of $E(Q)_{Aniline}$. The reaction of the Na^+ form gives a time course showing a rapid initial phase for the appearance of $E(Q)_{Aniline}$ that accounts for approximately 72.4% of the total amplitude. This fast phase is followed by a slower relaxation with $1/\tau \sim 3\ s^{-1}$. In contrast to this behavior, the reaction of the Cs^+ form occurs on a time scale where almost all of the $E(Q)_{Aniline}$ (97.6%) appears within the mixing dead-time of the stopped-flow apparatus. This burst appearance of $E(Q)_{Aniline}$ is followed by a slower phase of relatively small amplitude in which more $E(Q)_{Aniline}$ is formed. When lower aniline concentrations are used (1 or 0.2 mM, Figure 5), the yields of $E(Q)_{Aniline}$ are reduced, reflecting the reversible (*44*) and concentration-dependent nature of these reactions. However, the burst phase for all three forms of the enzyme is still complete within the mixing dead time of the stopped-flow apparatus (~1 ms).

DISCUSSION

A Hypothesis To Explain the Spectrum of the Tryptophan Synthase E(A−*A) Species.* Figure 6 presents the spectra of the tryptophan synthase L-Ser external aldimine and α-aminoacrylate species measured for the monovalent cation ion free (A), Na^+-bound (B), and Cs^+-bound (C) forms of the enzyme. The binding of Na^+ (Figure 6B) gives a distribution of the L-Ser external aldimine and α-aminoacrylate species in comparable amounts (*52*). The MVC-free enzyme gives predominantly α-aminoacrylate (*50*−*52*, *59*) (Figure 6A). Peracchi et al. (*43*) have shown that the binding of Cs^+ further perturbs the spectrum, forming a distinct absorption band at 460 nm that is postulated to be a Cs^+-bound α-aminoacrylate species. Also shown in Figure 6 and Table 1 are the log-normal curve fittings of the external aldimine and α-aminoacrylate spectra. As shown by Hur et al. (*65*) for the Na^+ form of the enzyme, after correction for light scattering, the 325−550 nm region of spectra containing both external aldimine and α-aminoacrylate can be fit by summing log-normal peaks with $\lambda_{max} = 460$, 424, and 350 nm. Owing to the compexity of the absorption spectra below 325 nm, the log-normal fitting of the spectra shown in Figure 6 is limited to the bands observed at wavelengths greater than 325 nm. Inclusion of bands for peaks at shorter wavelenges has only a minor effect on the amplitudes of the band at 350 nm (data not shown). The peak at 424 nm undoubtedly corresponds to the observed 425 nm peak of the external aldimine (*23*, *66*), and the 350 nm peak has been assigned as an α-aminoacrylate Schiff base species (*23*). It is noteworthy that the long-wavelength band that appears in the Cs^+-bound α-aminoacrylate (Figure 6C) coincides with the 460 nm log-normal curve used to fit the long-wavelength shoulder of the spectrum obtained in the reaction of the internal aldimine with L-Ser (Figure 6A) (*65*).

The unusual UV/Vis absorption spectrum of the tryptophan synthase α-aminoacrylate species, with λ_{max} 350 nm and a shoulder extending beyond 500 nm (Figure 1B and Figure 6), presents an interesting contrast with the spectra assigned to the α-aminoacrylate species of CBS and OASS (*34*−*38*). The CBS and OASS α-aminoacrylate spectra, with $\lambda_{max} =$ 460 and 470 nm, respectively, reflect the incorporation of an additional carbon−carbon double bond in conjugation with the PLP chromophore [structure $E(A-A)H^+$, Scheme 2], thus causing a red-shifting of the spectrum by 30−40 nm relative to the corresponding external aldimine species. The long-wavelength shoulder of the tryptophan synthase α-aminoacrylate likely arises from a structurally similar species. The perturbation of this spectrum induced by Cs^+ binding appears to be the consequence of a Cs^+-driven redistribution of enzyme-bound intermediates to slightly increase the fraction of 460 nm absorbing α-aminoacrylate species (*43*) (Figure 6). This 460 nm band is distinctly different in bandwidth, band shape, and intensity from quinonoid species formed in the tryptophan synthase reactions with substrates and substrate analogues (see Figure 1) (*5*, *24*, *44*, *45*, *59*, *67*, *68*), and is similar to the OASS and CBS α-aminoacrylates with respect to band shape. Therefore, the assignment of the 460 nm band to an α-aminoacrylate structure with a protonated Schiff base nitrogen, structure $E(A-A)H^+$, and the 350 nm band to an α-aminoacrylate

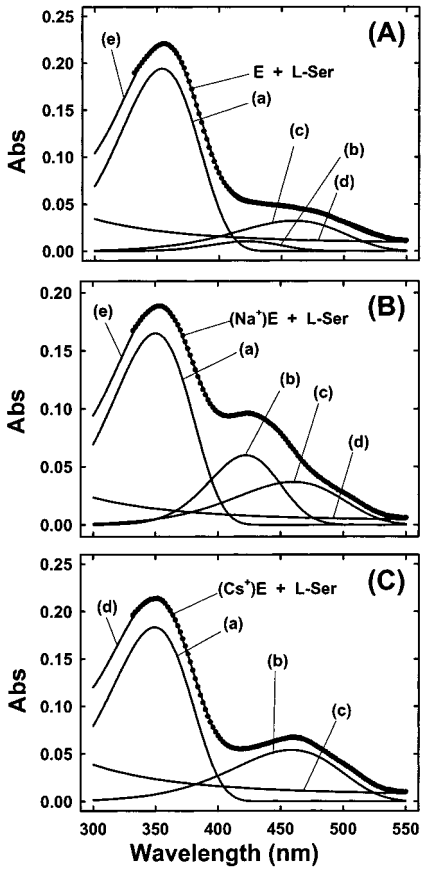

FIGURE 6: log-normal fitting of the tryptophan synthase $E(Aex_1)$ and E(A−A) UV/Vis absorption spectra measured for the monovalent cation ion free (A), Na^+-bound (B), and Cs^+-bound forms (C) of the enzyme. The dotted curve is the experimentally observed spectrum. In panels A and B, curve e is the sum of the curves for the individual bands (a−c) and the scattering curve (d). In panel C, the experimental data (dotted curve) could be fit with a curve (d) comprised of the sum of two absorption bands (a and b) plus the scattering curve (c). The fitting parameters for these log-normal fits are summarized in Table 1.

Table 1: log-normal Peak Fit Analyses of UV/Vis Static Absorbance Spectra Presented in Figure 5

samples[a]	curve[b]	amplitude[c] (Abs)	skewness[d] (nm)	bandwidth[e] (nm)	λ_{max}[f] (nm)
E + L-Ser (monovalent cation free)	a	0.194	0.77	76.35	354
	b	0.010	0.87	66.60	422
	c	0.032	0.76	103.00	460
E + L-Ser + Na^+	a	0.165	0.75	76.83	350
	b	0.060	0.87	66.61	422
	c	0.037	0.76	103.00	460
E + L-Ser + Cs^+	a	0.183	0.75	77.21	349
	b	0.054	0.76	103.08	459

[a] Samples are described in the caption to Figure 5 and in the text. [b] Curve designations refer to Figure 5. [c] Amplitudes at the band λ_{max} measured in absorbance units. [d] For convenience, skewness values have been converted from wavenumbers to nanometers in the table. Skewness values given in nanometers are <1.0 for a log-normal curve. The equation for skewness in wavenumbers is give by $\rho = (\nu_v - \nu_0)/(\nu_0 - \nu_r)$, where ν_0 is the wavenumber corresponding to λ_{max} and ν_v and ν_r are the wavenumber values at half-height on the "violet" and "red" sides of the curve, respectively. [e] The width of the curve at half-height in units of nanometers. [f] The maximum of the curve in nanometers (*25*, *52*−*55*).

Scheme 2: Protonated and Unprotonated Forms of the α-Aminoacrylate Schiff Base Intermediate[a]

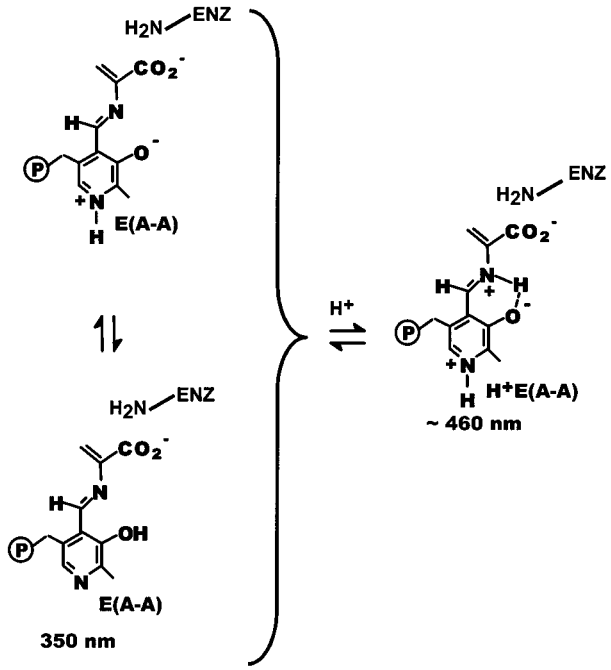

[a] Two tautomeric states of the unprotonated form are shown.

structure with a deprotonated Schiff base nitrogen, structure E(A−A) (Scheme 2), appears to be the most reasonable explanation. If these assignments are correct, then Cs^+ binding shifts the distribution of α-aminoacrylate species slightly in favor of the protonated form, thus giving rise to the 460 nm band apparent in Figure 6C.

The Conversion of the External Aldimine to the α*-Aminoacrylate Releases a Proton.* The phenol red rapid kinetic studies of the reaction presented in Figure 2 (weakly buffered with 1 mM substrate L-Ser) show two phases: a fast phase proton release that corresponds in rate to the formation of the L-Ser external aldimine, and a slower phase that corresponds in rate to the conversion of the external aldimine to the α-aminoacrylate interemediate. It is likely that the proton release in the fast phase is associated with the deprotonation of the L-Ser α-ammonium ion group as binding and conversion to the external aldimine occurs. The proton release in the slow phase establishes that the conversion of the Na^+ form of the L-Ser external aldimine to the α-aminoacrylate is accompanied by the release of H^+. The yield of H^+, estimated as illustrated in Figure 4, corresponds to about 0.5 proton per β-site for the kinetic relaxation corresponding to this conversion. Since the equilibrium distribution of enzyme-bound species is not completely dominated by the α-aminoacrylate, it appears that the apparent stoichiometry of proton release is about one per site under the conditions of the experiment. Hence, the conversion of the Na^+ form of the external aldimine to the α-aminoacrylate should be written according to eq 4, below:

Scheme 3: Thermodynamic Cycle for the Interconversion of the L-Ser External Aldimine and α-Aminoacrylate Schiff Base Intermediates

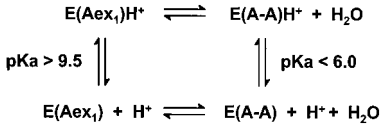

$$(Na^+)E(Aex_1)H^+ \rightleftarrows (Na^+)E(A-A) + H_2O + H^+ \quad (4)$$

Since the spectral assignments discussed above propose that the tryptophan synthase external aldimine Schiff base has a different protonation state than the predominating (350 nm) form of the α-aminoacrylate Schiff base, it then is reasonable to assign the proton release to this change in protonation state, as indicated in eq 4. The release of H^+ with a stoichiometry near one per site implies a sizable pK_a perturbation at the Schiff base nitrogen for the external aldimine to α-aminoacrylate interconversion, as depicted in Scheme 3:

This pK_a perturbation can be partially explained by the introduction of the conjugated $\alpha-\beta$ double bond. The replacement of the external aldimine hydroxymethyl group by this conjugated carbon−carbon double bond in the α-aminoacrylate should reduce the basicity of the Schiff base nitrogen and hence its pK_a. A second contribution could result from a change in the protein microenvironment in the vicinity of the Schiff base nitrogen as a consequence of the change in conformation from the more open structure of the external aldimine to the closed structure of the α-aminoacrylate.

Solution kinetic and spectroscopic studies of the various MVC-bound forms of tryptophan synthase have demonstrated that the conversion of the L-Ser external aldimine to the α-aminoacrylate is accompanied by a change in the β-subunit from an open to a closed conformation (Scheme 4) in which access to the β-site from solution is blocked (*44*, *50*−*52*, *59*, *61*−*63*, *69*−*72*). The nature of this conformational change is now fairly well characterized by structural studies (*13*−*15*, *42*). In the open conformation of the internal aldimine, one face and the edge of the PLP ring at C-4′ are exposed to solvent. This structure would allow the binding of L-Ser and nucleophilic attack of the L-Ser amino group at the C-4′ carbon. Solution studies indicate that when the external aldimine Schiff base is formed, there is a confor-

Scheme 4[a]

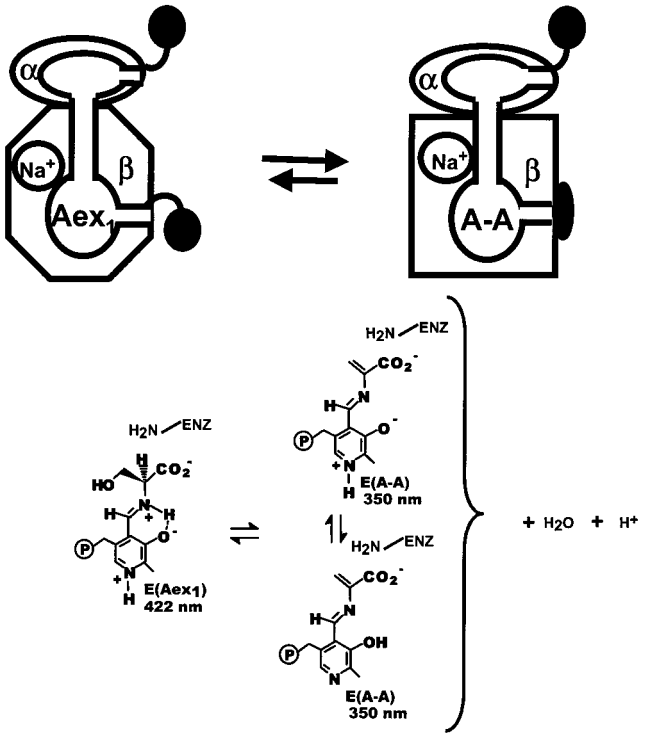

[a](A) Cartoon depicting interconversion of the partially closed, $E(Aex_1)$, and closed, E(A−A), conformations of an $\alpha\beta$-dimeric unit of the tryptophan synthase bienzyme complex. (B) Organic structures of the PLP cofactor for the interconversion of L-Ser external aldimine and α-aminoacrylate Schiff base intermediates.

mational transition to a partially closed state of the β-site (*70*), while the transition to the closed conformation occurs as the external aldimine is converted to the α-aminoacrylate. In the transition to the closed β-site conformation, domains in the β-subunit rotate relative to one another, blocking access from solution to the PLP ring and the α-aminoacrylate moiety. This conformation change is accompanied by the formation of a salt bridge between βD305 and βR141 (*72*, *73*) that forms part of the "lid" over the PLP ring (Scheme 4). This conformational transition causes the microenvironment of the Schiff base nitrogen to be less polar, and thereby likely decreases the pK_a of the protonated species.

These effects may not be sufficient to account for the large change in pK_a implied by the proton release stoichiometry (Figures 2 and 4) and the spectroscopic and kinetic data presented in Figures 5 and 6. Kagamiyama's group (*74*, *75*) have postulated that the large pK_a shifts seen in the external and internal aldimine species of transaminases arise from torsional effects at the C-4−C-4′ bond in the internal aldimine intermediate that distort the planar conformation of the aldimine structure and lower the pK_a (relative to the planar structure). Structural studies support the existence of these distorted structures both in aspartate aminotransferase and in aromatic amino acid transaminase. These distortions appear to arise from a combination of electrostatic and steric effects at the site. We spectulate that similar torsional effects may be important in the tryptophan synthase system. If the α-aminoacrylate Schiff base were distorted from planarity by changing the torsional angle about the C-4−C-4′ bond to a nonplanar structure, then the pK_a of the Schiff base nitrogen could be significantly lowered. However, the structure of the α-aminoacrylate complex is insufficiently well resolved in the region of the cofactor to determine if this distortion occurs (*42*). Nevertheless, the description of the electron density assigned to the aminoacrylate moiety in this structure is not inconsistent with this interpretation (*42*).

Interconversion of the 350 and 460 nm α-Aminoacrylate Species Is Rapid. Deprotonation of the imine nitrogen of the α-aminoacrylate provides a mechanism for decreasing the reactivity of the Schiff base linkage and the conjugated $\alpha-\beta$ double bond. The unprotonated (350 nm absorbing) α-aminoacrylate species could represent a deactivated, resting form of the enzyme. According to this argument, the 460 nm form of the α-aminoacrylate should be the more reactive species toward nucleophiles, and conversion of $(Na^+)E(A-A)$ to $(Na^+)E(A-A)H^+$ would activate the conjugated double bond for nucleophilic attack at C-β. If the interconversion of the 350 and 460 nm forms is slower than nucleophilic attack, then under conditions where the two forms preexist, $E(Q)_{Aniline}$ formation would occur in two kinetically distinct phases. If the interconversion is faster than nucleophilic attack, then $E(Q)_{Aniline}$ formation would occur in a single phase.

In the reaction of 10 mM aniline with preformed α-aminoacrylate (Figure 5)(eq 5), $E(Q)_{Aniline}$ formation is multiphasic with most of the reaction occurring in the mixing dead time. The small yield of $E(Q)_{Aniline}$ formed with the

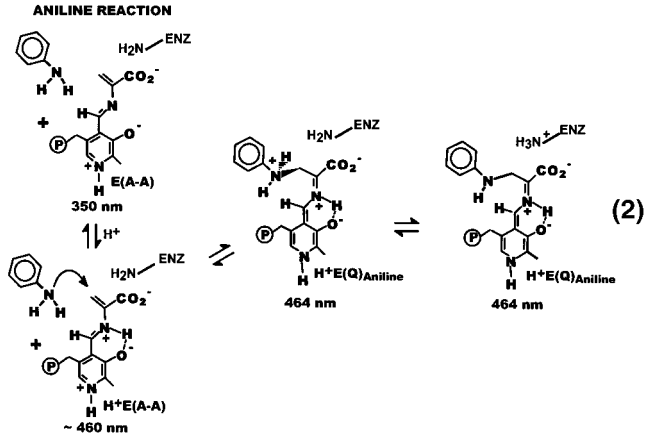

MVC-free enzyme (Figure 5A) is consistent with the requirement for MVC activation of the enzyme (*52*). With the Na^+ form of the enzyme (Figure 5B), approximately 72% of the $E(Q)_{Aniline}$ formed appears within the mixing dead-time, whereas with the Cs^+ form (Figure 5C), approximately 98% appears within the mixing dead-time. The slow residual relaxation present in the Na^+ system ($\sim$3 s^{-1}) occurs at a rate that is similar to the rate of conversion of the L-Ser external aldimine to the α-aminoacrylate (Figures 2 and 3), and the amplitude of this relaxation is consistent with that expected for conversion of the external aldimine initially present (Figure 6B) to $E(Q)_{Aniline}$. Consequently, any interconversion of the 350 and 460 nm α-aminoacrylate species appears to occur within the mixing dead-time. The Cs^+ form gives a slow relaxation of very small amplitude (2.4% of the total) with a rate of about 3 s^{-1}. This relaxation also is likely due to the conversion of a residual amount of external aldimine to $E(Q)_{Aniline}$.

Implications of the Absence of a Change in Protonation during the Aniline Reaction. The kinetic data presented in

Scheme 5

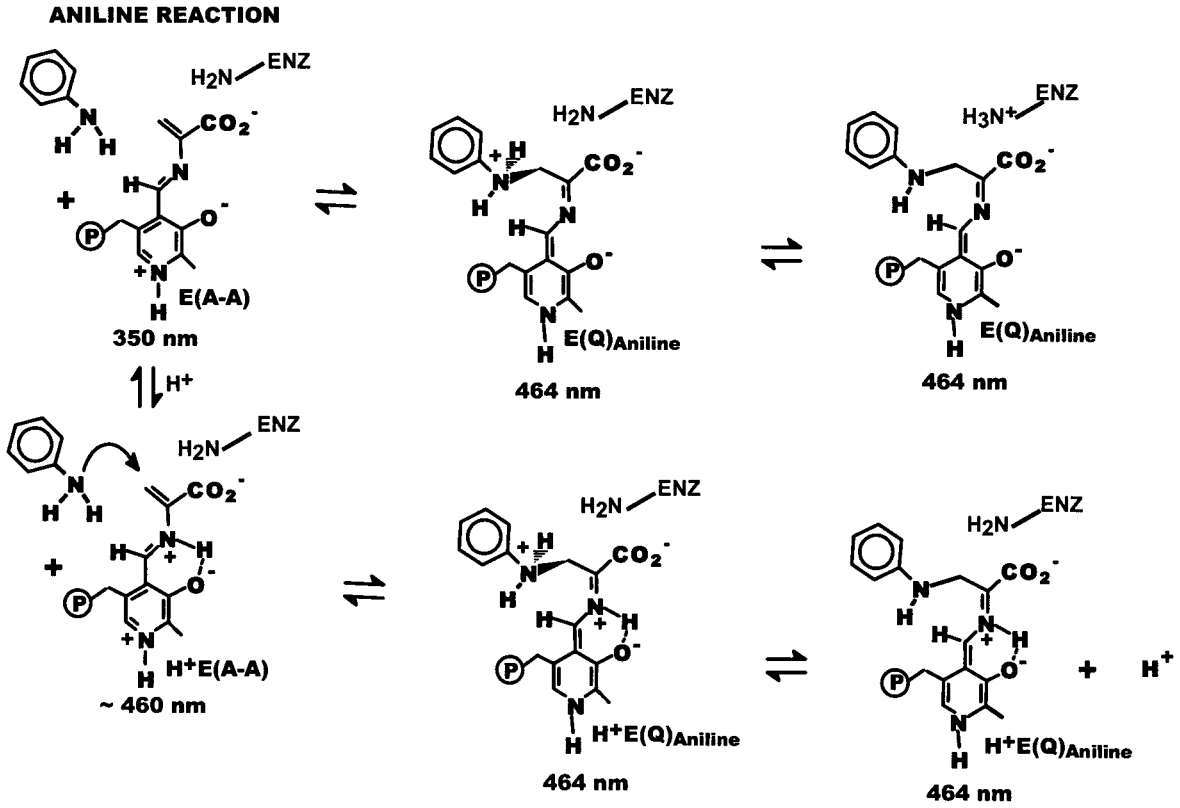

Figure 3 establish that there is no net change in H^+ attributable to the nucleophilic attack of aniline on the α-aminoacrylate to form $E(Q)_{Aniline}$. If this reaction involves the nucleophilic attack of the aniline nitrogen on the β-carbon of the unprotonated $(Na^+)E(A-A)$ species, then a quinonoid species should be formed wherein the aniline nitrogen is protonated and the imine nitrogen attached to the PLP C-4′ carbon remains unprotonated (Scheme 5). In a subsequent transfer, the proton from the aniline N-1 could be transferred to an acid−base catalytic group at the site (presumably βLys 87). These events would account for the absence of any detectable proton release. Alternatively, if $(Na^+)E(A-A)H^+$ is the more reactive, albeit minor, species, then nucleophilic attack could require the uptake of a proton to convert $(Na^+)E(A-A)$ to $(Na^+)E(A-A)H^+$ as reaction consumes $(Na^+)E(A-A)H^+$; however, this uptake could be compensated by loss of a proton from aniline, resulting in no net change in H^+.

Tryptophan synthase quinonoid species detected either as transients along the catalytic path (*23*, *24*) or as quasi-stable species derived from substrate analogues (such as aniline in this study) (*44*, *46*) give absorption spectra that are considerably blue-shifted relative to the quinonoid species detected with other PLP enzyme systems. The tryptophan synthase quinonoid species generally give intense absorption bands of narrow bandwidth in the 460−476 nm region of the spectrum, whereas most other PLP enzymes for which quinonoid intermediates have been detected give species with similarly intense bands and band shapes that are located at greater than 500 nm. Consequently, it is possible that the blue-shifted spectra of the tryptophan synthase quinonoid species arise from structures where, like the $(Na^+)E(A-A)$ species, the dominating species is not protonated at the imine nitrogen.

REFERENCES

1. Yanofsky, C., and Crawford, I. P. (1972) in *The Enzymes* (Boyer, P. D., Ed.) 3rd ed., pp 1−31, Academic Press, New York.
2. Davis, L., and Metzler, D. E. (1972) *Enzymes (3rd Ed.) 7*, 33−74.
3. Dunathan, H. C., and Voet, J. G. (1974) *Proc. Natl. Acad. Sci. U.S.A. 71*, 3888−3891.
4. Snell, E. E. (1975) *Adv. Enzymol. Relat. Areas Mol. Biol. 42*, 287−333.
5. Miles, E. W. (1979) *Adv. Enzymol. Relat. Areas Mol. Biol. 49*, 127−186.
6. Miles, E. W. (1986) Pyridoxal phosphate enzymes catalyzing β-elimination and β-replacement reaction. in *Pyridoxal Phosphate and Derivatives* (Dolphin, D., Poulson, R., and Avramovic, O., Eds.) pp 253−310, Wiley, New York.
7. Miles, E. W., Ahmed, S. A., and Kayastha, A. M. (1991) in *Enzymes dependent on pyridoxal phosphate and other carbonyl compounds as cofactors; proceeding of the 8th international symposium on vitamin B6 and carbonyl catalysis* (Fukui, T., Kagamiyama, H., Soda, K., and Wada, H., Eds), pp 249−256, Pergamon Press, New York.
8. Metzler, D. E. (2001) in *Biochemistry: The Chemical Reactions of Living Cells*, 2nd ed., pp 740−753, Harcourt/Academic Press, Burlington, MA.
9. Yano, T., Hinoue, Y., Chen, V. J., Metzler, D. E., Miyahara, I., Hirotsu, K., and Kagamiyama, H. (1993) *J. Mol. Biol. 234*, 1218−1229.
10. Onuffer, J. J., and Kirsch, J. F. (1994) *Protein Eng. 7*, 413−424.
11. Jhee, K.-H., Yang, L.-H, Ahmed, S. A., McPhie, P., Rowlett, R., and Miles, E. W. (1998) *J. Biol. Chem. 273*, 11417−11422.
12. Schnackerz, K. D. (1986) in *Pyridoxal Phosphate: Chemical Biochemical, and Medical Aspects, Part A* (Dolphin, D., Poulsen, R., and Avramovic, O., Eds.) pp 245−264, Wiley and Sons, New York.
13. Hyde, C. C., Ahmed, S. A., Padlan, E. A., Miles, E. W., and Davies, D. R. (1988) *J. Biol. Chem. 263*, 17857−17871.
14. Rhee, S., Parris, K. D., Ahmed, S. A., Miles, E. W., and Davies, D. R. (1996) *Biochemistry 35*, 4211−4221.
15. Rhee, S., Parris, K. D., Hyde, C. C., Ahmed, S. A., Miles, E. W., and Davies, D. R. (1997) *Biochemistry 36*, 7664−7680.
16. Scarsdale, J. N., Kazanima, G., Radaev, S., Schirch, V., and Wright, H. T. (1999) *Biochemistry 38*, 8347−8358.

17. Jager, J., Moser, M., Sauder, U., and Jansonius, J. N. (1994) *J. Mol. Biol. 239*, 285−305.
18. Peisach, D., Chipman, D. M., Van Ophem, P. W., Manning, J. M., and Ringe, D. (1998) *Biochemistry 37*, 4958−4967.
19. Jansonius, J. N. (1998) *Curr. Opin. Struct. Biol. 8*, 759−769.
20. Harris, C. M., Johnson, R. J., and Metzler, D. E. (1976) *Biochim. Biophys. Acta 421*, 181−194.
21. Metzler, C. M., Cahill, A., and Metzler, D. E. (1980) *J. Am. Chem. Soc. 102*, 6075−6082.
22. Mitra and Metzler, D. E. (1988) *Biochim. Biophys. Acta 965*, 93−96.
23. Drewe, W. F., Jr., and Dunn, M. F. (1985) *Biochemistry 24*, 3977−3987.
24. Drewe, W. F., Jr., and Dunn, M. F. (1986) *Biochemistry 25*, 2494−2501.
25. Metzler, C. M., Viswanath, R., and Metzler, D. E. (1991) *J. Biol. Chem. 266*, 9374−9381.
26. Braunstein, A. E. (1973) *Enzymes (3rd Ed.) 9*, 379−481.
27. Metzler, D. E., Harris, C. M., Johnson, R. J., and Siano, D. B. (1973) *Biochemistry 12*, 5377−5392.
28. Kallen, R. G., Korpela, T., Martell, A. E., Matsushima, Y., Metzler, C. M., Metzler, D. E., Morozov, Y. V., Ralston, I. M., Savin, F. A., Torchinsky, Yu. U., and Ueno, H. (1985) in *Transaminases* (Christen, P., and Metzler, D. E., Eds.) pp 37−108, John Wiley and Sons, New York.
29. Metzler, C. M., and Metzler, D. E, (1987) *Anal. Biochem. 166*, 313−327.
30. Goldberg, M. E., and Baldwin, R. L. (1967) *Biochemistry 6*, 2113−2119.
31. Mozzarelli, A., Peracchi, A., Rossi, G. L., Ahamed, S. A., and Miles, E. W. (1989) *J. Biol. Chem. 264*, 15774−15780.
32. Peracchi, A., Bettati, S., Mozzarelli, A., Rossi, G. L., Miles, E. W., and Dunn, M. F. (1996) *Biochemistry 35*, 1872−1880.
33. Jhee, K. H., McPhie, P., Ro, H. S., and Miles, E. W. (1998) *Biochemistry 37*, 14591−14604.
34. Jhee, K.-H., Niks, D., McPhie, P., Dunn, M. F., and Miles, E. W. (2001) *Biochemistry 40*, 10837−10880.
35. Tai, C.-H., and Cook, P. F. (2000) *Adv. Enzymol. Relat. Areas Mol. Biol. 74*, 185−234.
36. Tai, C.-H., and Cook, P. F. (2001) *Acc. Chem. Res. 34*, 49−59.
37. Woehl, E. U., Tai, C.-H., Dunn, M. F., and Cook, P. F. (1996) *Biochemistry 35*, 4776−4783.
38. Cook, P. F., and Wedding, R. T. (1976) *J. Biol. Chem. 251*, 2023−2029.
39. Cook, P. F., Hara, S., Nalabolu, S., and Schnackerz, K. D. (1992) *Biochemistry 31*, 2298−2303.
40. York, S. (1972) *Biochemistry 11*, 2733−2740.
41. Miles, E. W., Houck, D. R., and Floss, H. G. (1982) *J. Biol. Chem. 257*, 14203−14210.
42. Schneider, T. R., Gerhardt, E., Lee, M., Liang, P.-H., Anderson, K. S., and Schlichting, I. (1998) *Biochemistry 37*, 5394−5406.
43. Peracchi, A., Mozzarelli, A., and Rossi, G. L. (1995) *Biochemistry 34*, 9459−9465.
44. Dunn, M. F., Aguilar, V., Brzovic, P. S., Drewe, W. F., Jr., Houben, K. F., Leja, C. A., and Roy, M. (1990) *Biochemistry 29*, 8598−8607.
45. Roy, M., Keblawi, S., and Dunn, M. F. (1988) *Biochemistry 27*, 6698−6704.
46. Dunn, M. F., Roy, M., Robustell, B., and Aguilar, V. (1987) in *Proceedings of the 1987 International Congress on Chemical and Biological Aspect of Vitamin B6 Catalysis* (Korpela, T., and Christen, P., Eds.) pp 171−181, Birkhauser Verlag, Basel, Switzerland.
47. Kawasaki, H., Bauerle, R., Zon, G., Ahmed, S. A., and Miles, E. W. (1987) *J. Biol. Chem. 262*, 10678−10683.
48. Miles, E. W., Kawasaki, H., Ahmed, S. A., Morita, H., Morita, H., and Nagata, S. (1989) *J. Biol. Chem. 264*, 6288−6296.
49. Yang, L.-H., Ahmed, S. A., and Miles, E. W. (1996) *Protein Expression Purif. 8*, 126−136.
50. Woehl, E. U., and Dunn, M. F. (1999) *Biochemistry 38*, 7118−7130.
51. Woehl, E. U., and Dunn, M. F. (1999) *Biochemistry 38*, 7131−7141.
52. Woehl, E. U., and Dunn, M. F. (1995) *Biochemistry 34*, 9466−9476.
53. Houben, K. F., and Dunn, M. F. (1990) *Biochemistry 29*, 2421−2429.
54. Metzler, C. M., Cahill, A., Petty, S., Metzler, D. E., and Lang, L. (1985) *Appl. Spectrosc. 39*, 333−339.
55. Siano, D., and Metzler, C. M. (1969) *J. Chem. Phys. 51*, 1856−1861.
56. Dunn, M. F. (1974) *Biochemistry 13*, 1146−1151.
57. Maniscalco, S. J., Saha, S. K., Vicedomine, P., and Fisher, H. F. (1996) *Biochemistry 35*, 89−94.
58. Rowlett, R. S., and Silverman, D. N. (1982) *J. Am. Chem. Soc. 104*, 6737−6741.
59. Weber-Ban, E. U., Banik, U., Hur, O., Bagwell, C., Miles, E. W., and Dunn, M. F. (2001) *Biochemistry 40*, 3497−3511.
60. Roy, M., Keblawi, S., and Dunn, M. F. (1988) *Biochemistry 27*, 6698−6704.
61. Brzovic, P. S., Kayastha, A. M., Miles, E. W., and Dunn, M. F. (1992a) *Biochemistry 31*, 1180−1190.
62. Brzovic, P. S., Ngo, K., and Dunn, M. F. (1992b) *Biochemistry 31*, 3831−3839.
63. Brzovic, P. S., Hyde, C. C., Miles, E. W., and Dunn, M. F. (1993) *Biochemistry 32*, 10404−10413.
64. Sund, H., and Thoerell, H. (1962) *Enzymes, 2nd Ed. 7*, 26.
65. Hur, O., Leja, C., and Dunn, M. F. (1996) *Biochemistry 35*, 7378−7386.
66. Miles, E. W., and McPhie, (1974) *J. Biol. Chem. 249*, 2852−2857.
67. Phillips R. S., Miles, E. W., and Cohen, L. A. (1984) *Biochemistry 23*, 6228−6234.
68. Lane, A. N., and Kirschner, K. (1981) *Eur. J. Biochem. 120*, 379−387.
69. Leja, C. A., Woehl, E. U., and Dunn, M. F. (1995) *Biochemistry 34*, 6552−6561.
70. Pan, P., and Dunn, M. F. (1996) *Biochemistry 35*, 5002−5013.
71. Pan, P., Woehl, E., and Dunn, M. F.(1997) *Trends Biochem. Sci. 22*, 22−27.
72. Ferrari, D., Yang, L.-H., Miles, E. W., and Dunn, M. F. (2001) *Biochemistry 40*, 7421−7432.
73. Ferreari et al., in preparation.
74. Hayashi, H., Mizuguchi, H., and Kagamiyama, H. (1998) *Biochemistry 37*, 15076−15085.
75. Islam, M. M., Hayashi, H., Mizuguchi, H., and Kagamiyama, H. (2000) *Biochemistry 39*, 15418−15428.

BI025568U